Observation of Narrow-Band Terahertz Coherent Cherenkov Radiation from a Cylindrical Dielectric-Lined Waveguide

A. M. Cook,[1,*] R. Tikhoplav,[1] S. Y. Tochitsky,[2] G. Travish,[1] O. B. Williams,[1] and J. B. Rosenzweig[1]
[1]*Department of Physics and Astronomy, University of California, Los Angeles, California 90095, USA*
[2]*Department of Electrical Engineering, University of California, Los Angeles, California 90095, USA*
(Received 20 March 2009; published 27 August 2009)

We report experimental observation of narrow-band coherent Cherenkov radiation driven by a subpicosecond electron bunch traveling along the axis of a hollow cylindrical dielectric-lined waveguide. For an appropriate choice of dielectric wall thickness, a short-pulse beam current profile excites only the fundamental mode of the structure, producing energetic pulses in the terahertz range. We present detailed measurements showing a narrow emission spectrum peaked at 367 ± 3 GHz from a 1 cm long fused silica capillary tube with submillimeter transverse dimensions, closely matching predictions. We demonstrate a 100 GHz shift in the emitted central frequency when the tube wall thickness is changed by 50 μm. Calibrated measurements of the radiated energy indicate up to 10 μJ per 60 ps pulse for an incident beam charge of 200 pC, corresponding to a peak power of approximately 150 kW.

DOI: 10.1103/PhysRevLett.103.095003 PACS numbers: 52.59.Rz, 07.57.Hm, 41.60.Bq, 41.75.Lx

Modern electron accelerators show great promise as tools for creating radiation in the terahertz (THz) spectral region, conventionally defined as the range between 100 GHz and 30 THz [1]. A typical scenario involves the passage of an electron beam through a perturbing element such as a bend magnet, undulator, foil, or other structure that causes it to radiate [2,3]. The structure under present study, diagrammed in Fig. 1, is a hollow cylindrical dielectric tube coated on the outer surface with metal to form a dielectric-lined waveguide (DLW). As a relativistic electron bunch travels along the vacuum channel in the tube, it drives coherent Cherenkov radiation (CCR) wakefields [4] that are confined to a discrete set of modes due to the waveguide boundaries [5]. This slow-wave structure supports modes with phase velocity equal to the beam velocity that are thus capable of efficient energy exchange with the beam. With a sufficiently short (rms bunch length σ_z less than a radiation wavelength λ) driving beam containing N electrons, the radiation is coherent and its energy at the relevant longer wavelengths is enhanced by a factor proportional to N over incoherent radiation [6]. This coherent excitation process offers a simple and effective energy conversion scheme, allowing creation of sources producing unprecedented peak power at THz frequencies.

The use of DLW structures to convert the energy in an electron beam into radiation has been explored since the late 1940s [7]. Related experimental work has centered on particle acceleration (dielectric wakefield accelerator) [8,9] and microwave or THz generation [Cherenkov free-electron laser (CFEL) [10]]. The first operation of a CFEL at far-infrared wavelengths (375–1000 μm) was reported by Garate *et al.* in 1987, producing 10–200 kW pulses in a self-amplified configuration [11]. Walsh *et al.* subsequently demonstrated resonator operation at $\lambda = 100$ μm [12], and seeded amplifier operation has been demonstrated in the X band [13].

The experiment described in this Letter is based on a different excitation scenario, in which a short beam drives a coherent, single-mode wakefield in a DLW without a FEL gain process or microbunching instability. Our measurements demonstrate generation of THz-range pulses in a structure significantly shorter than a typical high-gain CFEL saturation length [14], at a power level comparable to that achieved in the aforementioned experiments. We further demonstrate how the method could be used to generate tens of megawatts of peak power at frequencies well above 1 THz using the kind of ultrashort electron beams that are available at current facilities. Although this method has been used previously to generate wakefields at microwave [15] and THz frequencies [16], these experiments have not measured the radiation directly. This Letter presents the first direct observation of THz-range radiation produced in this manner and demonstrates reasonable efficiency of energy extraction from the beam for a short structure (0.5% in 1 cm), highlighting the flexible utility for existing beam lines where high-power, beam-synchronized THz pulses of specific frequency and duration may be needed.

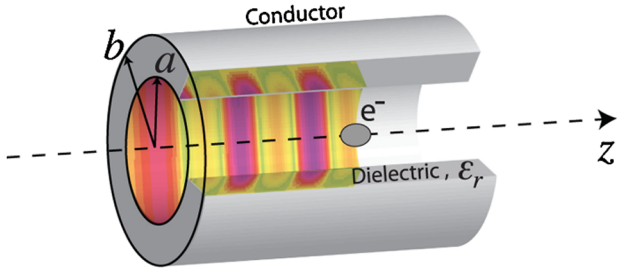

FIG. 1 (color online). Cutaway diagram of beam-driven cylindrical dielectric-lined waveguide. Color map illustrates longitudinal wakefield.

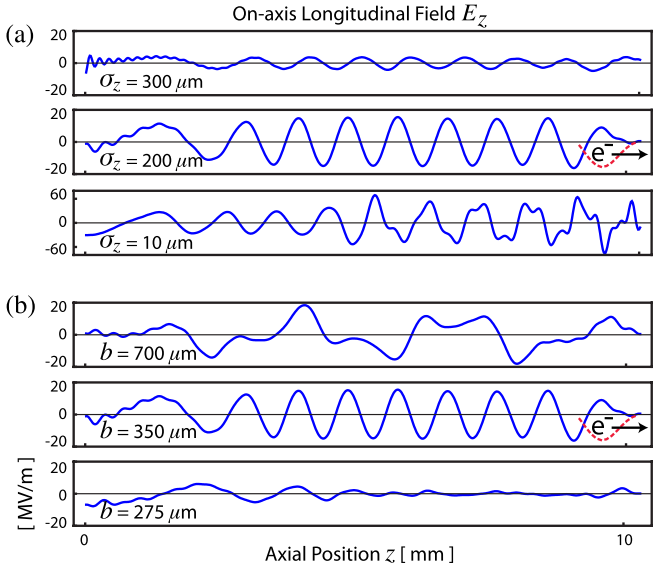

FIG. 2 (color online). OOPIC simulation of longitudinal wakefield E_z on tube axis versus position along tube, for (a) increasing σ_z with fixed $(a, b) = (250, 350)$ μm and (b) increasing b with fixed $(a, \sigma_z) = (250, 200)$ μm. Electron bunch is at the right edge of each plot, and has moved from left to right.

The dispersion equation describing the transverse modes of the DLW structure, for the azimuthally symmetric TM_{0n} case, is given by [17,18]

$$\frac{I_1(k_{0n}a)}{I_0(k_{0n}a)} = \frac{\varepsilon_r k_{0n}}{\kappa_{0n}} \frac{J_0(\kappa_{0n}b)Y_1(\kappa_{0n}a) - Y_0(\kappa_{0n}b)J_1(\kappa_{0n}a)}{Y_0(\kappa_{0n}a)J_0(\kappa_{0n}b) - Y_0(\kappa_{0n}b)J_0(\kappa_{0n}a)}, \quad (1)$$

where k_{0n} and κ_{0n} are the radial wave numbers in the vacuum and dielectric regions, respectively, ε_r is the relative permittivity of the material, and $n = 1, 2, 3, \ldots$ indexes the solutions to the transcendental equation. $J_m(x)$ and $Y_m(x)$ are Bessel functions of the first and second kinds of order m, and $I_m(x)$ is the modified Bessel function of the first kind. The frequencies of the excited modes are found from Eq. (1) using the fact that they have phase velocity equal to the beam velocity βc. For a given driving electron bunch length, the DLW tube dimensions (a, b) can be chosen such that only the TM_{01} mode is coherently excited, thus selecting a single operating frequency.

The electromagnetic simulation code OOPIC PRO [19] was used to conduct a design study of the tube structures, taking as free parameters a, b, ε_r, and σ_z. In Fig. 2, the simulated longitudinal electric field E_z at $r = 0$ is plotted along the length of the structure for the ideal case of an azimuthally symmetric beam traveling on the axis; results from several parameter configurations offer a picture of the qualitative structure of the excited wakefield. The plots in Fig. 2(a) illustrate the loss of coherence at $\lambda \approx 800$ μm as the bunch length is set beyond the value given by the roll-off wavelength condition $\lambda \gtrsim 2\pi\sigma_z$ for an ideal Gaussian axial charge distribution. The plots in Fig. 2(b) show the excitation of additional modes as the outer radius is increased to accommodate longer wavelengths; the scaling of these mode frequencies with b is shown in Fig. 3(a).

The driving electron beam parameters, belonging to the Neptune advanced accelerator laboratory at UCLA, are listed in Table I. The minimum bunch length achievable by the Neptune chicane compressor system has been previously established at $\sigma_z \lesssim 200$ μm (0.6 ps) [20] and confirmed in our measurements. This restriction informed the choice of radii (a, b) combinations of $(250, 350)$ and $(250, 400)$ μm, for which the TM_{01} mode wavelength is long enough to be coherently excited by the beam. For optimizing the radiated energy, a small inner radius [Fig. 3(b)] as well as a long tube length are desirable. An a value of 250 μm and length of 1 cm were chosen as the configuration that would produce the most energy while still allowing passage of the electron bunch through the structure. The dielectric tubes used in the measurements were obtained from 10 cm lengths of drawn fused silica ($\varepsilon_r = 3.8$) capillary, a material chosen for its universal availability. The tubing was coated with an outer layer of gold $\sim$1 μm thick over a $\sim$50 Å chromium adhesion layer, and then cleaved into 1 cm lengths. The Cr adhesion layer is necessary to prevent flaking of the Au coating during cleaving.

A schematic of the experiment is shown in Fig. 4. The incoming compressed electron beam is focused strongly into a dielectric tube by a triplet of permanent magnet quadrupoles. Downstream of the tube, the rapidly diverging beam and emitted CCR propagate collinearly to a 90° off-axis parabolic mirror (OAP), where the electron beam is dumped and the radiation is collimated out of the vacuum chamber into a detection apparatus. Circular waveguide elements immediately following the tube serve to

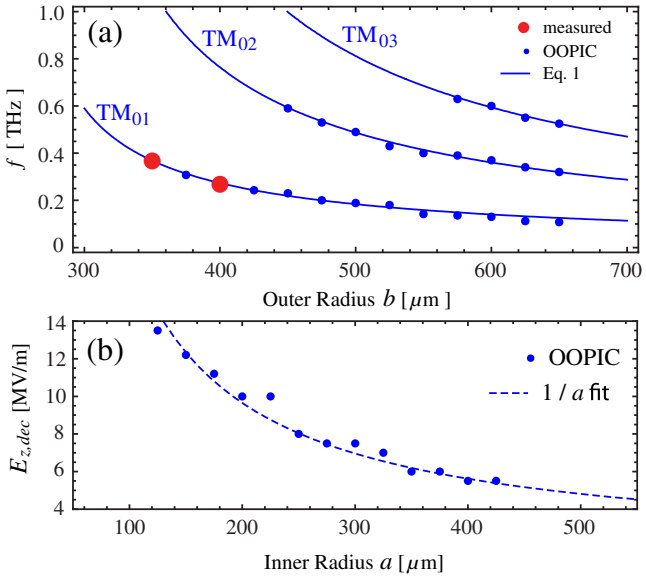

FIG. 3 (color online). (a) Scaling of mode frequencies with outer radius b, for constant $a = 250$ μm and $\sigma_z = 200$ μm. (b) Scaling of decelerating electric field, seen by driving electron bunch, with inner radius a.

TABLE I. Experimental parameters.

Bunch charge	Q	200 pC
rms bunch length	σ_z	200 μm
rms bunch radius	σ_r	80 μm
β function		1 cm
Beam energy		10–11 MeV
Dielectric inner radius	a	250 μm
Dielectric outer radius	b	350, 400 μm
Dielectric tube length	L	1 cm
Dielectric constant	ε_r	3.8

control the diverging THz beam and ultimately direct the radiation forward from a horn antenna toward the OAP mirror. Coherent transition radiation (CTR) produced when the electron beam strikes the OAP and coherent diffraction radiation (CDR) excited as it passes the end of the dielectric structure present measurable backgrounds; the signal-to-noise ratio of CCR to CTR and CDR is established at roughly 9:1 by measuring the energy emitted when the beam passes through a steel ''dummy tube'' and comparing it to that of a dielectric tube.

Measurement of the CCR power spectrum was accomplished by autocorrelating the radiation pulse and applying discrete Fourier transform analysis to the data. An example of the raw autocorrelation data, taken using a standard Michelson interferometer in conjunction with a cryogenically cooled bolometer detector, is shown in Fig. 5(a). The interferogram is clearly oscillatory over a relatively long time scale, in stark contrast to the characteristic lone central peak that would arise from the broadband CTR and CDR background. Spectra from two tubes of differing outer radii, shown in Fig. 5(b), indicate narrow emission peaks close to the design frequencies of 368 and 273 GHz. The measured frequency results are summarized and compared with predictions in Table II, which includes calculations for a higher-frequency structure that was not tested due to fabrication difficulties. The error estimates quoted are the standard deviation of central frequency values from several different autocorrelation scans. A shift of $\sim$100 GHz in the central frequency is observed between tubes, which agrees well with predictions and demonstrates

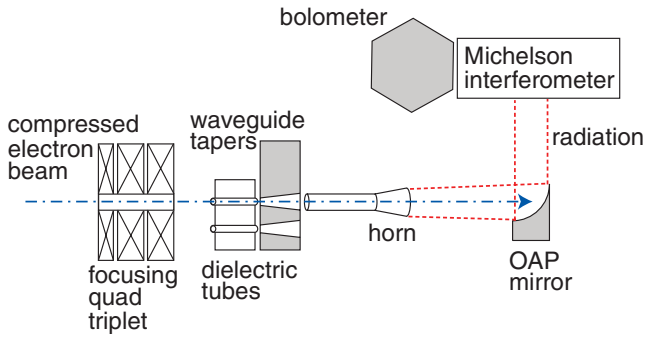

FIG. 4 (color online). Schematic of experimental setup.

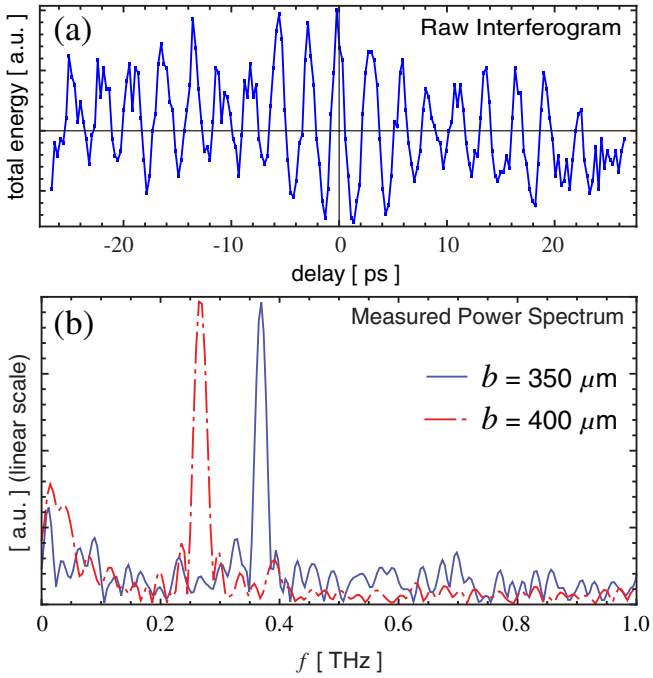

FIG. 5 (color online). (a) Typical measured partial autocorrelation interferogram of radiation from $b = 350$ μm tube. (b) Measured power spectra, calculated by discrete Fourier transform, of radiation from $b = 350$ and 400 μm tubes. Low-frequency hump represents CTR and CDR background.

effective tunability. While the structures used in this study are designed to operate at under 0.5 THz, availability of a shorter electron beam ($\sigma_z \lesssim 25$ μm, as was achieved in previous DLW field-induced breakdown experiments at SLAC [16]) would enable use of tubes designed for frequencies well above 1 THz.

Table II also contains calculated frequencies of the lowest-order TE and hybrid (HEM) modes supported by the structures, found analytically using dispersion equations analogous to Eq. (1). It is reasonable to assume that the driving electron beam was off axis by some amount and azimuthally asymmetric, and thus would excite hybrid modes; however, the strong coupling of the beam to the TM_{01} mode excitation through the large E_z field on axis appears to dominate any contribution of HEM modes.

The 3 dB bandwidth of the central peak observed in each spectrum is $\sim$15–50 GHz, depending on the length of the autocorrelation scan. A scan that observes the end of the

TABLE II. Comparison of measured mode frequencies with predictions, for different tube sizes.

	$b = 400$ μm	$b = 350$ μm	$b = 325$ μm
Measured TM_{01}	268 $\pm$ 2 GHz	367 $\pm$ 3 GHz	—
OOPIC PRO TM_{01}	266 GHz	365 GHz	445 GHz
Analytical TM_{01}	273 GHz	368 GHz	450 GHz
Analytical TE_{01}	387 GHz	541 GHz	693 GHz
Analytical HEM_{11}	248 GHz	355 GHz	456 GHz

radiation pulse indicates that the full duration, which is set by the tube length, is greater than 60 ps. The majority of the autocorrelation traces obtained are partial scans, due to hardware limitations, and therefore the spectra give an upper limit on the bandwidth.

The total CCR energy emitted was measured by removing the interferometer device and focusing the radiation directly into a calibrated Golay cell detector. For an incident bunch charge of ~200 pC, these measurements detect up to 10 μJ of energy per pulse after subtraction of background, as compared to the 2 mJ total carried by the electron beam. This corresponds to a peak power of 150 kW for a radiation pulse 60 ps long. Simulation estimates put the emitted energy at ~15 μJ, a discrepancy that is reasonable considering the losses present in the quasioptical transport.

We now consider structure variations that would give improved results when paired with other existing beams. For example, with a 0.5 nC beam as short as $\sigma_z \approx 20$ μm such as that at the SLAC LCLS facility [21], a tube of a suitably transparent material (e.g., high-density polyethylene) [22] with $a = 50$ μm, $b = 80$ μm, and $L = 10$ cm would radiate at 1.8 THz with ~0.1% bandwidth. Relative to the experimental case, the higher beam charge, shorter bunch length, and smaller inner tube radius [Fig. 3(b)] contribute to greater radiation power $P \propto N^2 \exp(-4\pi^2\sigma_z^2/\lambda^2)$; the total radiated energy would be an estimated 30 mJ (OOPIC), accounting for absorption losses, which corresponds to a peak power on the order of 50 MW in a 450 ps-long pulse. This is more than an order of magnitude greater than that currently produced by synchrotron [2] and FEL [23] THz sources, as well as sources based on optical rectification [24] and frequency mixing [25]. This CCR source would provide a unique THz pump for experiments using the FEL x-ray beam as a probe [26]. The use of DLW structures at high power is limited by an electric breakdown threshold, which, e.g., for fused silica tubing is found experimentally to be ~13.8 GV/m (at dielectric surface) [16]. The case for the LCLS beam presented here is within this limit, neglecting to consider sub-breakdown material degradation effects and possible lowering of breakdown threshold due to long-pulse exposure.

We have reported the first direct measurements of THz-range Cherenkov radiation driven by a subpicosecond electron beam in a dielectric wakefield structure. Our results demonstrate the potential of this method as a flexible source of step-tunable, narrow-band, multimegawatt peak-power radiation at $f > 1$ THz for use in existing electron accelerators.

This work was supported by the U.S. Department of Energy, Offices of High Energy Physics (Contracts No. DE-FG03-92ER40693, No. DE-FG03-92ER40727) and Basic Energy Sciences (Contract No. DE-FG02-07ER46272), and the Office of Naval Research (Contract No. N00014-06-1-0925). The authors acknowledge the help of D. Haberberger, J. Sarrett, M. Thompson, P. Musumeci, and A. Knyazik.

*alancook@ucla.edu

[1] M. Tonouchi, Nat. Photon. **1**, 97 (2007).
[2] G. Carr, M. Martin, W. McKinney, K. Jordan, G. Neil, and G. Williams, Nature (London) **420**, 153 (2002).
[3] S. Korbly, A. Kesar, J. Sirigiri, and R. Temkin, Phys. Rev. Lett. **94**, 054803 (2005).
[4] P. A. Cherenkov, Phys. Rev. **52**, 378 (1937).
[5] J. D. Jackson, *Classical Electrodynamics* (Wiley, New York, 1999) 3rd ed.
[6] J. Nodvick and D. Saxon, Phys. Rev. **96**, 180 (1954).
[7] V. L. Ginsburg, Dokl. Akad. Nauk SSSR **56**, 253 (1947).
[8] W. Gai, P. Schoessow, B. Cole, R. Konecny, J. Norem, J. Rosenzweig, and J. Simpson, Phys. Rev. Lett. **61**, 2756 (1988).
[9] J. Power *et al.*, Phys. Rev. ST Accel. Beams **3**, 101302 (2000).
[10] J. Walsh, T. Marshall, M. Mross, and S. Schlesinger, IEEE Trans. Microwave Theory Tech. **25**, 561 (1977).
[11] E. Garate *et al.*, Nucl. Instrum. Methods Phys. Res., Sect. A **259**, 125 (1987).
[12] J. Walsh *et al.*, Nucl. Instrum. Methods Phys. Res., Sect. A **272**, 132 (1988).
[13] E. Garate, H. Kosai, K. Evans, A. Fisher, R. Cherry, and W. Main, Appl. Phys. Lett. **56**, 1092 (1990).
[14] V. Asgekar and G. Dattoli, Opt. Commun. **206**, 373 (2002).
[15] P. Schoessow, M. Conde, W. Gai, R. Konecny, J. Power, and J. Simpson, J. Appl. Phys. **84**, 663 (1998).
[16] M. Thompson *et al.*, Phys. Rev. Lett. **100**, 214801 (2008).
[17] H. P. Freund and A. K. Ganguly, Nucl. Instrum. Methods Phys. Res., Sect. A **296**, 462 (1990).
[18] T.-B. Zhang, T. Marshall, and J. Hirshfield, IEEE Trans. Plasma Sci. **26**, 787 (1998).
[19] D. L. Bruhwiler *et al.*, Phys. Rev. ST Accel. Beams **4**, 101302 (2001).
[20] S. Anderson, J. Rosenzweig, P. Musumeci, and M. Thompson, Phys. Rev. Lett. **91**, 074803 (2003).
[21] J. Arthur *et al.*, SLAC Report No. R-0521, 1998 (unpublished).
[22] M. Naftaly and R. Miles, J. Appl. Phys. **102**, 043517 (2007).
[23] N. Gavrilov *et al.*, Nucl. Instrum. Methods Phys. Res., Sect. A **575**, 54 (2007).
[24] F. Blanchard *et al.*, Opt. Express **15**, 13 212 (2007).
[25] S. Tochitsky, C. Sung, S. Trubnick, C. Joshi, and K. Vodopyanov, J. Opt. Soc. Am. B **24**, 2509 (2007).
[26] A. Cavalleri *et al.*, Nature (London) **442**, 664 (2006).